29th International Cosmic Ray Conference Pune (2005) **00**, 101–104

Evidence of an Inverse Compton Origin for the HESS Spectrum of G347.3−0.5

G.E. Allen[a], J.C. Houck[a], T.G. Pannuti[b], S.J. Sturner[c,d]

(a) Massachusetts Institute of Technology, Kavli Institute for Astrophysics and Space Research, 77 Massachusetts Avenue, NE80-6029, Cambridge, MA 02139-4307

(b) California Institute of Technology, Spitzer Science Center, MS 220-6, 1200 East California Blvd., Pasadena, CA 91125

(c) NASA Goddard Space Flight Center, Code 661, Greenbelt, MD 20771

(d) Universities Space Research Association, 7501 Forbes Boulevard, Suite 206, Seabrook, MD 20706-2253

Presenter: G.E. Allen (gea@space.mit.edu), usa-allen-G-abs2-og22-poster

Very-high–energy gamma-ray spectra of the supernova remnant G347.3−0.5 have been published by the *CANGAROO* and *HESS* collaborations. Several analyses of the *CANGAROO* data have been reported. Here we present the results of a joint spectral analysis of the *HESS* data, some *XMM* X-ray data and some *ATCA* radio data. The X-ray and radio data were fitted with a synchrotron radiation model. Inverse Compton scattering, nonthermal bremsstrahlung and neutral-pion decay models were considered for the gamma-ray data. Only the cosmic microwave background radiation is used as seed photons for the inverse Compton process. The results of these analyses suggest that the *HESS* spectrum is dominated by inverse Compton scattered photons.

1. Introduction

The supernova remnant G347.3−0.5 is one of only a few shell-type remnants reported to emit TeV gamma rays. Both the *CANGAROO* and *HESS* collaborations report the detection of TeV gamma-ray emission from the remnant [1, 2]. While some argue that the *CANGAROO* spectrum is produced by the decay of neutral pions, an extrapolation of the π^0 spectrum to GeV energies yields a flux that is too large to be consistent with the constraints derived from *EGRET* data [3] unless only the highest energy protons diffuse far enough away from the shock to interact in high-density material [4, 5, 6]. Alternatively, the *CANGAROO* spectrum might be described by inverse Compton scattering of the cosmic microwave background radiation, but this model is incompatible with the *CANGAROO* data [4] unless the volume filled by the very-high–energy electrons is at least one hundred times larger than the volume filled by the compressed or amplified magnetic field [5, 7].

2. Data and Analysis

This paper describes the results of a joint spectral analysis of some X-ray, gamma-ray and radio data for the supernova remnant G347.3−0.5. X-ray spectra for most of the remnant were obtained by analyzing data from four of five archived *XMM* observations. The fifth data set was excluded because the data are dominated by events associated with a background flare. Only data from the EPIC PN CCDs were included in the present analysis. The data were analyzed using the techniques described in the SAS Users' Guide. The fields of view of the four pointings do not span the entire extent of the supernova remnant. The fraction of the source flux in these fields was estimated using some archived *ROSAT* PSPC data. Since 71% of the total number of events associated with the source (after background subtraction) are in the four fields, the normalizations of the models used to fit the X-ray data are multiplied by a factor of 1.40 (i.e. 1/0.71).

The radio flux densities at 1.4 and 2.5 GHz (6.7 ± 2.0 and 5.6 ± 1.7 Jy, respectively) obtained from *ATCA* data [5] are included in the joint spectral fits. Although these results are only for the bright northwestern rim, the

Table 1. Parameters of the models jointly fitted to some *XMM*, *HESS* and *ATCA* data

Quantity	Inverse Compton	Nonthermal Bremsstrahlung
$n_{\rm H}^{\rm NW}$ [10^{21} cm^{-2}]	6.19 ± 0.09	6.19 ± 0.09
$n_{\rm H}^{\rm SW}$ [10^{21} cm^{-2}]	7.11 ± 0.11	7.11 ± 0.11
$n_{\rm H}^{\rm SE}$ [10^{21} cm^{-2}]	5.50 ± 0.15	5.50 ± 0.15
$n_{\rm H}^{\rm C}$ [10^{21} cm^{-2}]	3.79 ± 0.10	3.79 ± 0.10
Γ	1.96 ± 0.05	1.96 ± 0.05
ϵ [TeV]	23^{+8}_{-5}	30^{+37}_{-14}
B [μG]	20^{+16}_{-8}	13^{+29}_{-10}
${\rm Norm}_{\rm X}^{\rm NW}$ [cm^{-2}]	$1.2^{+1.9}_{-0.5} \times 10^3$	$2.5^{+27.5}_{-2.1} \times 10^4$
${\rm Norm}_{\rm X}^{\rm SW}$ [cm^{-2}]	$8.3^{+13}_{-5.2} \times 10^3$	$1.7^{+18.3}_{-1.5} \times 10^4$
${\rm Norm}_{\rm X}^{\rm SE}$ [cm^{-2}]	$4.4^{+6.6}_{-2.7} \times 10^3$	$8.9^{+101}_{-7.6} \times 10^3$
${\rm Norm}_{\rm X}^{\rm C}$ [cm^{-2}]	$3.4^{+5.2}_{-2.1} \times 10^3$	$6.9^{+76}_{-5.9} \times 10^3$
${\rm Norm}_{\rm G}$ [cm^{-2}]	$1.4^{+0.8}_{-0.6} \times 10^5$	$5.7^{+2.4}_{-2.0} \times 10^6$
${\rm Norm}_{\rm R}$ [cm^{-2}]	4.0×10^4	8.0×10^4
χ^2/dof	10190/3759	10190/3759

The spectral parameters include the interstellar absorption column ($n_{\rm H}$), the differential spectral index of the electron spectrum at 1 GeV (Γ), the exponential cut-off energy of the electron spectrum (ϵ), the total magnetic field strength (B) and the normalizations of the X-ray (${\rm Norm}_{\rm X}$), gamma-ray (${\rm Norm}_{\rm G}$) and radio (${\rm Norm}_{\rm R}$) spectra. The absorption column density was allowed to vary separately for the northwestern (NW), southwestern (SW), southeastern (SE) and central (C) X-ray data sets. The spectral index, curvature and cut-off energy were fixed to be the same for each data set. The magnetic field strength was fixed to be the same for each of the X-ray and radio data sets. The normalization was allowed to vary separately for each of the X-ray and gamma-ray data sets. The radio normalization was fixed to be ${\rm Norm}_{\rm R} = 1.40({\rm Norm}_{\rm X}^{\rm NW} + {\rm Norm}_{\rm X}^{\rm SW} + {\rm Norm}_{\rm X}^{\rm SE} + {\rm Norm}_{\rm X}^{\rm C})$. The statistical uncertainties are quoted at the 90% confidence level.

flux densities are assumed to represent the radio emission from the entire remnant because the emission from the feature designated as "Arc 2" in Figure 5 of [5] may not be associated with G347.3−0.5 [8].

The *HESS* spectral data used are based on the results depicted in Figure 3 of [2].

The spectral analyses were performed using the spectral-fitting package ISIS and the scripting language S-Lang. The nonthermal emission spectra are based on an electron spectrum that is a power law in momentum with an exponential cut off at very-high energies. The X-ray and radio data were fitted with a synchrotron radiation model. The X-ray flux was modified by an interstellar absorption column. The gamma-ray data were fitted with inverse Compton and nonthermal bremsstrahlung models. Only the cosmic microwave background radiation is used as seed photons for the inverse Compton process. The neutral-pion decay emissivity curve of [9] is used to estimate the properties of the remnant if the *HESS* emission is due to the decay of neutral pions. The results of the spectral fits are listed in Table 1 and displayed in Figure 1.

3. Discussion

The spectral data for the unidentified *EGRET* source 3EG J1714−3857 are shown in Figure 1. This source is the brightest source near G347.3−0.5, but may not be associated with the remnant. Therefore, the *EGRET* data points should be regarded as upper limits. Since none of the potential gamma-ray spectral models exceeds the *EGRET* data, it is not necessary to assume that only the very-highest–energy electrons (nonthermal

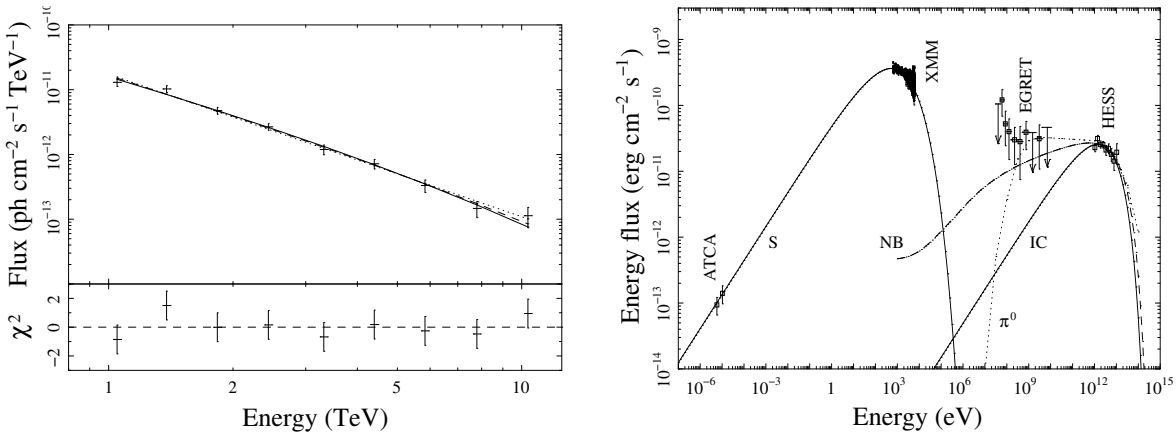

Figure 1. *Left*: The *HESS* spectrum for the entire remnant G347.3−0.5 [2]. The top panel shows the source spectrum (data points) and three models. The dotted line is the best-fit power law ($\chi^2/\mathrm{dof} = 6.59/7$). The solid curve is the best-fit inverse Compton model ($\chi^2/\mathrm{dof} = 4.70/7$). The dashed curve is the best-fit nonthermal bremsstrahlung model ($\chi^2/\mathrm{dof} = 5.08/7$). The bottom panel shows the differences between the data points and the inverse Compton model divided by the uncertainties in the data points. *Right*: A multiwavelength energy-flux spectrum for the entire remnant including some *ATCA*, *XMM*, *EGRET* and *HESS* data. Synchrotron (S), inverse Compton (IC), nonthermal bremsstrahlung (NB) and neutral pion decay (π^0) spectra are also shown.

bremsstrahlung) or protons (neutral-pion decay) diffuse far enough to interact with a high-density target for this reason.

The values of χ^2 (Table 1) do not provide a means of discriminating between different gamma-ray emission models. The fitted values for the differential spectral index and cut-off energy of the electron spectrum and for the magnetic field strength and absorption column density are reasonable for both the inverse Compton and nonthermal bremsstrahlung models. The only spectral parameters that may help determine the origin of the *HESS* flux are the gamma-ray and radio normalizations. For the inverse Compton model, the ratio of these two normalizations is 3.5 (1.1–11.4 at the 90% c.l.). This indicates that the inverse-Compton–emitting volume is 3.5 times larger than the synchrotron-emitting volume, which suggests that the very-high–energy electrons fill a volume that is 3.5 times larger than the volume filled by a high magnetic field strength. This condition seems plausible. Since the volume ratio is close to one and since TeV inverse Compton emission is produced by more or less the same electrons that produce X-ray synchrotron emission, the *HESS* image should be similar to the X-ray image, which is true [2].

If the *HESS* emission is produced by nonthermal bremsstrahlung, then the ratio of the gamma-ray and radio normalizations is 71 (5–550 at the 90% c.l.). This indicates that the density of protons $n_\mathrm{p} = 71(V_B/V_\mathrm{e})$, where V_B is the volume filled by the large magnetic field (i.e. the synchrotron-emitting volume) and V_e is the volume filled by the very-high–energy electrons (i.e. the nonthermal-bremsstrahlung–emitting volume). Since G347.3−0.5 exhibits little or no evidence of thermal X-ray emission [7, 11], the density of protons in the X-ray–emitting regions can be no larger than about 0.1 cm^{-3}. The density implied by the nonthermal bremsstrahlung model is about seven hundred times larger than this limit unless (1) the volume filled by the electrons is much larger than the volume filled by the magnetic field or (2) the highest energy electrons diffuse far enough away from the shock to interact in high-density molecular clouds that have not yet been heated by the shock. If the very-high–energy electrons fill a volume much larger than the volume filled by the magnetic

field, then the *HESS* image should be very different from (instead of similar to) the X-ray image. If the highest energy electrons are interacting in dense molecular clouds, then the *HESS* image should map the distribution of high-density material. Yet, the *HESS* image does not seem to be consistent with images of CO emission [12].

Although we did not fit the *HESS* data with a neutral-pion decay model, we used the emissivity curve of [9] to estimate that the density of the target protons would have to be $n_{\rm p} = 1900(a_{\rm e}/a_{\rm p})(V_B/V_{\rm p})$, where $a_{\rm e}/a_{\rm p}$ is the ratio of the number densities of electrons and protons at 1 GeV and $V_{\rm p}$ is the volume filled by the very-high–energy protons (i.e. the neutral-pion–emitting volume). If $a_{\rm p} \sim 100a_{\rm e}$, then the discussion regarding the nonthermal bremsstrahlung model applies equally well to the neutral-pion decay model.

4. Conclusions

We performed joint spectral analyses of the *HESS* data, some *XMM* X-ray data and some *ATCA* radio data for G347.3−0.5. The results of these analyses show that the gamma-ray models no longer violate the limits imposed by the *EGRET* data. If the gamma-ray emission is produced by nonthermal bremsstrahlung or the decay of neutral pions, then the target density must be at least about one hundred times larger than the limits on the proton density in the X-ray–emitting region. Yet the remarkable similarity of the *HESS* and X-ray images suggest that the *HESS* emission is produced in more or less the same region as the X-ray emission instead of being produced in, say, nearby molecular clouds, which have a different distribution on the sky. Therefore, it seems difficult to reconcile the nonthermal bremsstrahlung and neutral-pion decay models with the observed properties of the remnant. However, an inverse Compton origin for the *HESS* emission would easily explain the similarities of the *HESS* and X-ray images and the spectral results obtained for an inverse Compton model are reasonable. Therefore, it seems likely that the *HESS* emission is dominated by inverse Compton scattering of the cosmic microwave background radiation.

5. Acknowledgements

This work has benefited from the insights of a number of experts in the field. We gratefully acknowledge the useful suggestions of Chuck Dermer, Don Ellison, Tom Jones and Stephen Reynolds.

References

[1] H. Muraishi et al., Astron. Astrophys. 354, L57 (2000).
R. Enomoto et al., Nature. 416, 823 (2002).
[2] F. A. Aharonian et al., Nature. 432, 75 (2004).
[3] O. Reimer, O. and M. Pohl, Astron. Astrophys. 390, L43 (2002).
[4] Y. Uchiyama et al., Astron. Astrophys. 400, 567 (2003).
[5] J. S. Lazendic et al., Astrophys. J. 602, 271 (2004).
[6] M. A. Malkov et al., Astrophys. J. in press (2005).
[7] T. G. Pannuti et al., Astrophys. J. 593, 377 (2003).
[8] D. C. Ellison et al., Astrophys. J. 563, 191 (2001).
[9] T. K. Gaisser, Astrophys. J. 492, 219 (1998).
[10] R. C. Hartman et al., Astrophys. J. Suppl. Ser. 123, 79 (1999).
[11] G. Cassam-Chenaï et al., Astron. Astrophys. 427, 199 (2004).
[12] Y. Fukui et al., Publ. Astron. Soc. Jpn. 55, L61 (2003).